Accuracy analysis of the phase-screen propagator: implications for modeling and migration

Lian-Jie Huang and Michael C. Fehler, Los Alamos National Laboratory*

Summary

We present formal and numerical error analyses of the phase-screen (or split-step Fourier) propagator. Numerical results suggest that the propagator is accurate up to 60 degrees propagation angle relative the main propagation direction for media with small velocity perturbations. We investigate the errors from various approaches for splitting the exponential operator of the phase-screen propagator. The symmetrically split equations are slightly more accurate than the one-step split equations. Numerical examples show that the differences among splitting approaches are not significant. Therefore, relative to the symmetrically split equations, the one-step-free one-step-perturbation split equation is more efficient for migration in which wavefields in the space domain at all depth levels must be calculated. However, the half-step-free one-step-perturbation half-step-free split equation has almost the same efficiency as the one-step split equations for forward wave simulations.

Introduction

The phase-screen (or split-step Fourier) propagator has been used for modeling forward and reflected wave propagation (*e.g.* Wu and Huang, 1992; Wu *et al.*, 1995) and migration (*e.g.* Stoffa *et al.*, 1990; Huang and Wu, 1996). Cheng *et al.* (1996) gave a formal error analysis of the phase-screen propagator by defining a propagation angle in a reference medium and concluded that the propagation angle should be less than 40 degrees to control the error from expansion of the square-root operator to under 5%. However, we are interested in understanding how accurate the phase-screen propagator is for a given propagation angle in a real medium rather than in a reference medium. We analyze the error from expansion of the square-root operator and from splitting the exponential operator of the phase-screen propagator using the formal and numerical methods.

Expansion of the square-root operator

The one-way wave equation is given by

$$\frac{\partial}{\partial z} p(x, y, z; \omega) = i\mathcal{Q}p(x, y, z; \omega) \tag{1}$$

with the square-root operator $\mathcal{Q}$ defined by

$$\mathcal{Q} \equiv \sqrt{\frac{\omega^2}{v^2(x, y, z)} + \left(\frac{\partial^2}{\partial x^2} + \frac{\partial^2}{\partial y^2}\right)} \ , \tag{2}$$

where $p(x, y, z; \omega)$ is the pressure in the frequency domain, ω is the circular frequency, and $v(x, y, z)$ is the velocity of the medium. Equation (1) leads to the equation for wave-field extrapolation

$$p(x, y, z + \Delta z; \omega) = e^{i\Delta z \mathcal{Q}} p(x, y, z; \omega) \ , \tag{3}$$

where Δz is the vertical extrapolation interval.

In the phase-screen propagator (*cf.* Stoffa, *et al.*, 1990; Wu and Huang, 1992), by choosing a reference medium with a velocity $v_0(z)$, the square-root operator $\mathcal{Q}$ is approximated by

$$\mathcal{Q} \approx \mathcal{Q}' = \sqrt{k_0^2(z) + \left(\frac{\partial^2}{\partial x^2} + \frac{\partial^2}{\partial y^2}\right)} + k_0(z)\left[n(x, y, z) - 1\right] \ , \tag{4}$$

where $k_0(z) \equiv \omega / v_0(z)$ is the wavenumber in the reference medium, and $n(x, y, z) \equiv v_0(z)/v(x, y, z)$ is the refraction index.

Error from expansion of the square-root operator

To evaluate the error introduced by expansion of the square-root operator, we consider a homogeneous medium with a velocity $v(x, y, z) = const$. Making use of equation (2) and Fourier transforming equation (1) over x and y yields the equation for the Fourier transform of $\mathcal{Q}$ given by

$$\widetilde{\mathcal{Q}} = k\sqrt{1 - \left(\frac{k_T}{k}\right)^2} \ , \tag{5}$$

where $k = \omega/v$ is the wavenumber and $k_T = \sqrt{k_x^2 + k_y^2}$ is the transverse component of the wavenumber. Using equation (4) and Fourier transforming equation (1) over x and y leads to the equation for the Fourier transform of $\mathcal{Q}'$ given by

$$\widetilde{\mathcal{Q}'} = k\left[\sqrt{\frac{1}{n^2} - \left(\frac{k_T}{k}\right)^2} + \frac{1}{n}(n - 1)\right] \ . \tag{6}$$

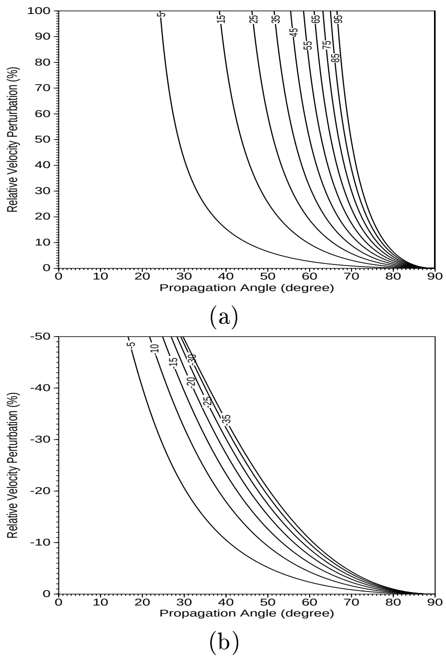

Figure 1: Contours of the relative error from expansion of the square-root operator versus propagation angle and relative velocity perturbation.

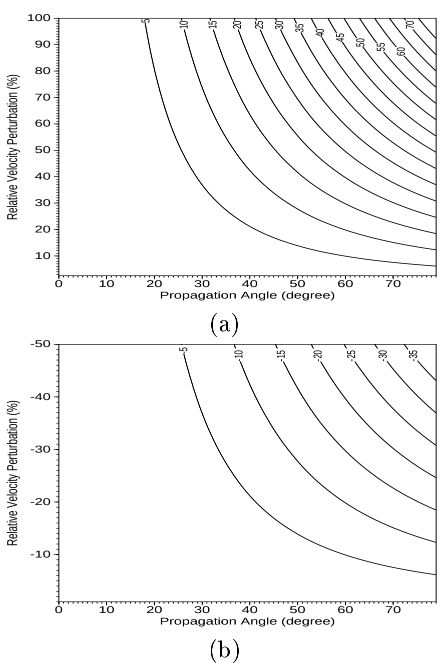

Figure 2: Contours of the relative traveltime error of the phase-screen propagator versus propagation angle and relative velocity perturbation.

For a plane wave propagating along a propagation angle θ relative to the main propagation direction z-axis, equation (5) becomes

$$\widetilde{\mathcal{Q}} = k\, cos\theta \ , \tag{7}$$

and equation (6) can be written as

$$\widetilde{\mathcal{Q}'} = k \left[\sqrt{\frac{1}{n^2} - sin^2\theta} + \frac{1}{n}(n-1) \right] \ . \tag{8}$$

For one-way wave propagation or migration problems, the angle θ is restricted by $0 \le \theta < 90$, and hence, $\widetilde{\mathcal{Q}} > 0$ if $\omega \neq 0$. The relative error defined by $E_r \equiv \left(\widetilde{\mathcal{Q}'} - \widetilde{\mathcal{Q}} \right) / \widetilde{\mathcal{Q}}$ is therefore given by

$$E_r(\theta, n) = \frac{1}{cos\theta} \left[\sqrt{\frac{1}{n^2} - sin^2\theta} + \frac{1}{n}(n-1) - cos\theta \right] \ . \tag{9}$$

In terms of the relative slowness perturbation $\delta n = n - 1$, equation (9) can be written as

$$E_r(\theta, \delta n) = \frac{1}{cos\theta} \left[\sqrt{\frac{1}{(1+\delta n)^2} - sin^2\theta} + \frac{\delta n}{1+\delta n} - cos\theta \right] \ . \tag{10}$$

Alternatively, E_r versus the relative velocity perturbation $\delta n_v \equiv (v - v_0)/v_0$ is given by

$$E_r(\theta, \delta n_v) = \frac{1}{cos\theta} \left[\sqrt{(1+\delta n_v)^2 - sin^2\theta} - \delta n_v - cos\theta \right] \ . \tag{11}$$

Equations (9)–(11) indicate that $E_r = 0$ if $\theta = 0$ for waves propagating along z-axis, or if $\delta n = 0$ (*i.e.* $n = 1$, $\delta n_v = 0$) for a homogeneous medium, as expected. The relative error contours versus the propagation angle θ and the relative velocity perturbation δn_v are displayed in Figure 1. The figure demonstrates that, the relative error caused by expansion of the square-root operator is $\pm 5\%$ when the propagation angles are about 40–45 degrees and the relative velocity perturbations are $\pm 10\%$. The propagation angles are shrunk to about 17–25 degrees when the relative velocity perturbations are either 100% or -50%.

To analyze the accuracy of the phase-screen propagator, relative traveltime errors of seismograms generated by the phase-screen method were calculated. A 2D homogeneous model defined on a grid 1024×100 was used. The grid spacings along x- and z-axis are both 10m. The velocity of the model is 4000m/s. A point source with a Ricker's time history and a dominant frequency 20Hz was introduced at grid point (512,1). The seismogram was recorded at each grid point from (512,100) to (512,1023), which corresponds to propagation angles ranging from 0 to 79 degrees relative to z-axis. Ideal seismograms were computed using an analytical solution. Seismograms were generated using the phase-screen propagator for relative velocity perturbations ranging from 2.5% to 100% with an interval of 2.5% for the case of positive perturbation, and ranging from -1% to -50% with an interval of -1% for the case of negative perturbation. Relative traveltime errors were computed for each calculation and their contours are shown in Figure 2. We see from Figure 2(a) and (b) that, for ±5% relative traveltime errors, the propagation angles are approximately 60 degrees when the relative velocity perturbations are ±10%, while the propagation angles are about 18–25 degrees when the relative velocity perturbations are either 100% or -50%. In general, numerical tests suggest that the phase-screen propagator can handle larger propagation angles than what are estimated by Figure 1 for given velocity perturbation and relative error levels.

Error from splitting the exponential operator

Substituting equation (4) into equation (3) yields

$$p(x, y, z + \Delta z; \omega) = e^{(\mathcal{A}+\mathcal{B})\Delta z} p(x, y, z; \omega) \ , \qquad (12)$$

where operators $\mathcal{A}$ and $\mathcal{B}$ are defined by

$$\mathcal{A} = i\, k_0(z) \left[n(x, y, z) - 1 \right] \ , \qquad (13)$$

$$\mathcal{B} = i \sqrt{k_0^2(z) + \left(\frac{\partial^2}{\partial x^2} + \frac{\partial^2}{\partial y^2} \right)} \ . \qquad (14)$$

Jensen *et al.* (1994) discussed the following different approaches for splitting the exponential operator,

$$\text{(I)}: \quad e^{(\mathcal{A}+\mathcal{B})\Delta z} \approx e^{\mathcal{A}\Delta z}\, e^{\mathcal{B}\Delta z} \ , \qquad (15)$$

$$\text{(II)}: \quad e^{(\mathcal{A}+\mathcal{B})\Delta z} \approx e^{\mathcal{B}\Delta z}\, e^{\mathcal{A}\Delta z} \ , \qquad (16)$$

$$\text{(III)}: \quad e^{(\mathcal{A}+\mathcal{B})\Delta z} \approx e^{\frac{\mathcal{A}}{2}\Delta z}\, e^{\mathcal{B}\Delta z}\, e^{\frac{\mathcal{A}}{2}\Delta z} \ , \qquad (17)$$

$$\text{(VI)}: \quad e^{(\mathcal{A}+\mathcal{B})\Delta z} \approx e^{\frac{\mathcal{B}}{2}\Delta z}\, e^{\mathcal{A}\Delta z}\, e^{\frac{\mathcal{B}}{2}\Delta z} \ . \qquad (18)$$

The terms with operator $\mathcal{B}$ are evaluated by a Fourier transform and the phase-screen marching solutions corresponding to each of the above four spitting approaches can be written as

$$p^{I}(z + \Delta z) = e^{a} \mathcal{F}^{-1} \left\{ e^{b} \mathcal{F} \left\{ p(z) \right\} \right\} \ , \qquad (19)$$

$$p^{II}(z + \Delta z) = \mathcal{F}^{-1} \left\{ e^{b} \mathcal{F} \left\{ p(z) e^{a} \right\} \right\} \ , \qquad (20)$$

$$p^{III}(z + \Delta z) = e^{\frac{a}{2}} \mathcal{F}^{-1} \left\{ e^{b} \mathcal{F} \left\{ p(z) e^{\frac{a}{2}} \right\} \right\} \ , \qquad (21)$$

$$p^{VI}(z + \Delta z) = \mathcal{F}^{-1} \left\{ e^{\frac{b}{2}} \mathcal{F} \left\{ e^{a} \mathcal{F}^{-1} \left[e^{\frac{b}{2}} \mathcal{F}[p(z)] \right] \right\} \right\} \ , \qquad (22)$$

where the variables x, y, and ω in the pressure functions have been omitted, $\mathcal{F}$ and $\mathcal{F}^{-1}$ represent respectively the forward and inverse Fourier transforms over x and y, $a \equiv i\, k_0\, (n-1)\Delta z$, and $b \equiv i\, k_{0z} \Delta z$ with $k_{0z} = \sqrt{k_0^2 - k_x^2 - k_y^2}$. Equations (19) and (20) are called the one-step split equations, while equations (21) and (22) are termed the symmetrically split equations. Equation (19) is also called the one-step-free one-step-perturbation split equation and equation (22) the half-step-free one-step-perturbation half-step-free split equation. Jensen *et al.* (1994) showed that the errors from splitting operator in the approaches (I) and (II) are second order in (Δz), while those from (III) and (IV) are third order in (Δz). Following Jensen *et al.* (1994), it can be shown that in equations (19)–(22) the errors from approximation of the integral in the exponential operator (*i.e.* the formal solution of one-way wave equation) are all in order $(\Delta z)^2$.

A 2D slice of the SEG/EAEG 3D salt model shown in Figure 3 was used to compare the accuracy between equations (19) and (22). The model was defined on a grid 1024×300 with a grid spacing 12.192m. A point source with a Ricker's time history and a dominant frequency 20Hz was introduced at the center of the upper boundary of the model. Seismograms calculated using equations (19) and (22) were recorded at the bottom of the model and are displayed respectively in Figure 4(a) and (b). The difference between Figure 4(a) and (b) as shown in Figure 4(c) is almost invisible. The relative difference is about 0.15%. Figure 4(d) shows the difference blown up by a factor of 10.

For forward wave propagation, the innermost Fourier transform and the outermost inverse Fourier transform in equation (22) are not necessary except the first and the last depth steps. The half-step-free propagation can be combined with that for the next depth level. Consequently, the computational efficiency of equation (22) becomes almost the same as that of equation (19) but equation (22) provides a slightly more accurate result than equation (19). However, these Fourier transforms in equation (22) are necessary for the migration where the wavefields for every depth level are required to produce images. Therefore, using equation (19) for migration is more efficient than using equation (22) while the accuracy for both equations are almost the same. Equation (21) requires an additional complex number multiplication relative to equation (19).

Conclusions

We have analyzed the error from expansion of the square-root operator using the formal method and compared the results with numerical tests. For large velocity perturbations (double velocity contrast), both formal and numerical error analyses suggest that the phase-screen propagator can handle wave propagation up to about 20 degrees relative to the main propagation direction z-axis with ±5% relative errors. For small velocity perturbations ($\leq 10\%$), the formal error analysis indicates that the phase-screen propagator can be used for simulating wave propagation up to about 45 degrees of propagation angle but numerical analysis demonstrates that the angle can be up to 60 degrees. We have analyzed and numerically verified the errors from splitting the exponential operator. The symmetrically split equations are a little more accurate than the one-step split equations. Numerical examples showed that the differences among splitting approaches are not significant. From the computational efficiency point of view, the one-step-free one-step-perturbation split equation is more suitable for migration since it provides almost the same accuracy as that of the symmetrically split equations. The half-step-free one-step-perturbation half-step-free split equation is almost as efficient as the one-step split equations for forward wave propagation problems.

Acknowledgements

This work is part of the Advanced Computational Technology Initiative. Funding came from the Department of Energy Office of Basic Energy Sciences through contract W-7405-ENG-36.

References

Cheng, N., Cheng, C. H., and Toksöz, M. N., 1996, Error analysis of phase screen method in 3-D: Geophys. Res. Lett., **23**, 1841–1844.

Huang, L.-J., and Wu, R.-S., 1996, Prestack depth migration with acoustic screen propagators: 66th Ann. Internat. Mtg., Soc. Expl. Geophys., Expanded Abstracts, 415–418.

Jesen, F. B., Kuperman W. A., Porter, M. B., and Schmidt, H., 1994, Computational ocean acoustics: AIP Press.

Stoffa, P. L., Fokkema, J. T., de Luna Freire, R. M., and Kessinger, W. P., 1990, Split-step Fourier migration: Geophysics, **55**, 410–421.

Wu, R.-S., and Huang, L.-J., 1992, Scattered field calculation in heterogeneous media using the phase-screen propagator: 62nd Ann. Internat. Mtg., Soc. Expl. Geophys., Expanded Abstracts, 1289–1292.

Wu, R.-S., Huang, L.-J., and Xie, X.-B., 1995, Backscattered wave calculation using the de Wolf approximation and a phase-screen propagator: 65th Ann. Internat. Mtg., Soc. Expl. Geophys., Expanded Abstracts, 1293–1296.

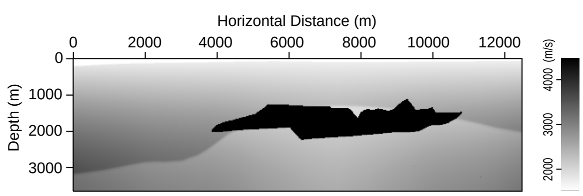

Figure 3: 2D slice of the SEG/EAEG 3D salt model.

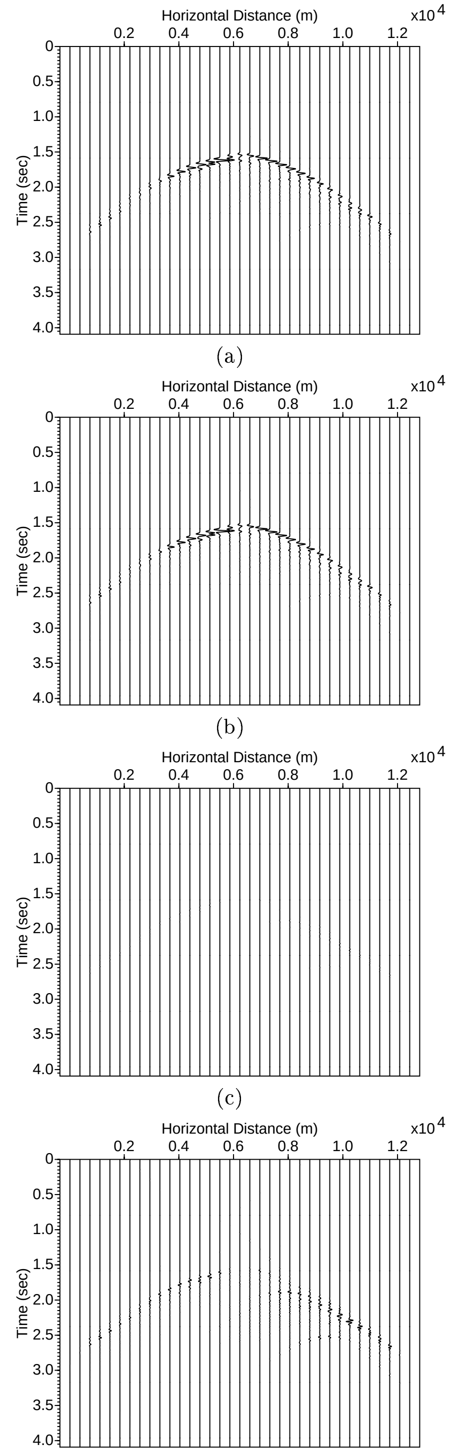

Figure 4: Comparison of seismograms calculated by the phase-screen propagators (a) with splitting approach (I), (b) with splitting approach (VI). (c) is the results of subtracting (b) from (a). (d) shows (c) multiplied by a factor of 10.